Title

Positron emission tomography harmonization in the Alzheimers Disease Neuroimaging Initiative: A scalable and rigorous approach to multisite amyloid and tau quantification.

Journal

Alzheimers & Dementia: The Journal of the Alzheimers Association, 21(1)

Authors

Landau, Susan

Harrison, Theresa

Baker, Suzanne

et al.

Publication Date

2025

DOI

10.1002/alz.14378

Peer reviewed

Received: 4 June 2024 | Revised: 7 October 2024 | Accepted: 10 October 2024

DOI: 10.1002/alz.14378

Alzheimer's & Dementia®
THE JOURNAL OF THE ALZHEIMER'S ASSOCIATION

RESEARCH ARTICLE

Positron emission tomography harmonization in the Alzheimer's Disease Neuroimaging Initiative: A scalable and rigorous approach to multisite amyloid and tau quantification

Susan M. Landau[1] | Theresa M. Harrison[1] | Suzanne L. Baker[2] | Martin S. Boswell[2] | JiaQie Lee[1] | Jacinda Taggett[1] | Tyler J. Ward[1] | Trevor Chadwick[1] | Alice Murphy[1] | Charles DeCarli[3] | Christopher G. Schwarz[4] | Prashanthi Vemuri[4] | Clifford R. Jack Jr.[4] | Robert A. Koeppe[5] | William J. Jagust[1,2] | for the U.S. POINTER Study Group and for the Alzheimer's Disease Neuroimaging Initiative

[1]Neuroscience Department, University of California, Berkeley, California, USA

[2]Molecular Biophysics and Integrated Bioimaging, Lawrence Berkeley National Laboratory, Berkeley, California, USA

[3]University of California, Davis, California, USA

[4]Department of Radiology, Mayo Clinic, Rochester, Minnesota, USA

[5]Department of Radiology, University of Michigan, Ann Arbor, Michigan, USA

Correspondence
Susan M. Landau, 118 Barker Hall MC #3190, UC Berkeley, Berkeley, CA 94720-3190, USA.
Email: slandau@berkeley.edu

Data used in preparation of this article were obtained from the Alzheimer's disease neuroimaging initiative (ADNI) database (adni.loni.usc.edu). As such, the investigators within the ADNI contributed to the design and implementation of ADNI and/or provided data but did not participate in analysis or writing of this report. A complete listing of ADNI investigators can be found at: http://adni.loni.usc.edu/wp-content/uploads/how_to_apply/ADNI_Acknowledgement_List.pdf

Funding information
Alzheimer's Disease Neuroimaging Initiative (ADNI); Alzheimer's Association, Grant/Award Number: U.S. POINTER-19-611541; National Institute on Aging; National Institute of Biomedical Imaging and Bioengineering; Takeda Pharmaceutical Company; Center for Alzheimer's and Related Dementias (CARD), Grant/Award Number: AG000546; National

Abstract

INTRODUCTION: A key goal of the Alzheimer's Disease NeuroImaging Initiative (ADNI) positron emission tomography (PET) Core is to harmonize quantification of β-amyloid (Aβ) and tau PET image data across multiple scanners and tracers.

METHODS: We developed an analysis pipeline (Berkeley PET Imaging Pipeline, B-PIP) for ADNI Aβ and tau PET images and applied it to PET data from other multisite studies. Steps include image pre-processing, refacing, magnetic resonance imaging (MRI)/PET co-registration, visual quality control (QC), quantification of tracer uptake, and standardization of Aβ and tau standardized uptake value ratios (SUVrs) across tracers.

RESULTS: Measurements from 10,105 cross-sectional and longitudinal Aβ and tau PET scans acquired in several studies between 2010 and 2024 can be processed, harmonized, and directly merged across tracers and cohorts.

DISCUSSION: The B-PIP developed in ADNI is a scalable image harmonization approach used in several observational studies and clinical trials that facilitates rigorous Aβ and tau PET quantification and data sharing.

KEYWORDS
Alzheimer's disease, Aβ PET, tau PET

Institutes of Health; NIH/NIA, Grant/Award Numbers: U24 AG072122, AG067418

Highlights

- Quantitative results from ADNI Aβ and tau PET data are generated using a rigorous, scalable image processing pipeline
- This pipeline has been applied to PET data from several other large, multisite studies and trials
- Quantitative outcomes are harmonizable across studies and are shared with the scientific community

1 | INTRODUCTION

Over the past 20 years, positron emission tomography (PET) imaging in Alzheimer's disease (AD) has grown from a specialized research approach used only in a handful of research centers to a more broadly accessible tool that has played a pivotal role in observational studies, clinical trials, and patient assessment.[1] This increased use has led to the need for acquisition and analysis approaches that are scalable, reproducible, and maximize measurement sensitivity and accuracy in the face of potential sources of noise and bias related to the use of multiple scanners and tracers. The Alzheimer's Disease Neuroimaging Initiative (ADNI) PET Core has aimed to meet these needs by developing tools for quantitative β-amyloid (Aβ) and tau PET analysis and making these data available to the scientific community.

In this study, we describe the ADNI PET Core processing stream for Aβ and tau image analysis (Berkeley PET Imaging Pipeline [B-PIP]) and its application to all ADNI baseline and longitudinal Aβ and tau PET scans acquired between 2010 and 2024. While B-PIP has evolved over time, a major emphasis has been the development of strategies that account for multisite and multitracer imaging. Key features of harmonization include standardized image acquisition and reconstruction parameters, followed by application of B-PIP image processing that results in a common spatial resolution and voxel size, quantitative tracer uptake outcomes using anatomically-defined regions, and harmonization of these quantitative data to account for different tracer characteristics. The primary pipeline involves quantification in native space using a contemporaneous MRI ("MRI-dependent") to define PET regions of interest (ROIs), but there is a parallel template space quantification pathway to accommodate PET scans without an available MRI ("MRI-free"). Resulting MRI-dependent or MRI-free standardized uptake value ratios (SUVrs) can be harmonized using tracer-specific linear transformations. Finally, Aβ PET SUVrs are converted to Centiloids (CL) using tracer-specific and region-specific equations developed for use with this pipeline. Tau PET standardization across tracers is still under development; several approaches are currently being evaluated and are compatible with future use with B-PIP.

B-PIP was developed in ADNI and the Berkeley Aging Cohort Study (BACS),[2] and has been adopted by other studies and trials. This effort has resulted in a large amount of harmonized quantitative Aβ and tau PET image outcomes that are directly comparable within and across studies, facilitating multicohort analyses. Here, we present all available ADNI Aβ and tau PET data alongside harmonized Aβ and tau PET data from several studies led by ADNI PET Core investigators, including the SCAN project (Standardized Centralized Alzheimer's & Related Dementias Neuroimaging), the U.S. POINTER imaging substudy (study to PrOtect brain health through lifestyle INTErvention to Reduce risk), and the BACS. Additional information related to harmonization (e.g., CL thresholds, conversion equations to account for tracer-related differences or use of an MRI for SUVr quantification) is provided. All of the image data presented in this paper have been acquired and processed using B-PIP, and all data are available to the scientific community. Finally, we describe future goals of the ADNI PET Core related to further multicohort image analysis, facilitating access to harmonized quantitative outcomes by the research community.

2 | METHODS

2.1 | Study design and cohorts

We analyzed Aβ and tau PET scans acquired in ADNI, POINTER Imaging, SCAN, and BACS that were available as of April 2024. Participant characteristics are described in Table 1 and each included cohort is described below. Protocols for each cohort were approved by local and central institutional review boards (IRBs), and written informed consent was obtained from all participants. Study cohorts included participants who had at least one Aβ and tau PET scan, with other cohort-specific inclusion or exclusion criteria noted below. To assess clinical status and cognitive performance, we used study-specific clinical diagnoses and, when available, the global Clinical Dementia Rating Scale (CDR) measured closest in time to the baseline Aβ and/or tau scan.

2.1.1 | ADNI

ADNI is a longitudinal natural history study of AD that includes a variety of neuroimaging, cognitive, and fluid biomarker assessments, and is designed to serve as a model for clinical trials.[3] Participants included individuals who had ≥ 1 Aβ PET scan with ^{18}F florbetapir (FBP) or ^{18}F florbetaben (FBB) and/or tau PET scans with [18F]Flortaucipir (FTP) and a contemporaneous MRI. ADNI participants are between ages 55

and 90 years at baseline, had completed at least 6 years of education, were fluent in Spanish or English, and were free of any other significant neurologic diseases. Individuals diagnosed with AD dementia and mild cognitive impairment (MCI) met standard diagnostic criteria and all CN participants (with or without a subjective cognitive complaint) had CDR scores of 0.[4] Longitudinal scans were available for 60% of individuals with a baseline Aβ scan and 47% of individuals with baseline tau scan (see Table 1).

2.1.2 | SCAN

The SCAN project[5] was conceived to harmonize processing of prospectively acquired PET and MRI scans from Alzheimer's disease research centers (ADRCs) across the US. ADRCs are funded by the National Institute on Aging (NIA) and carry out research on AD and related dementias in order to improve diagnosis, treatment, and patient care. A variety of neuroimaging and other biomarker data are acquired across ADRCs, and SCAN MRI and PET Cores have defined acquisition protocols and image analysis pipelines (described here for PET) that enable harmonization of imaging outcomes with other multisite studies, including ADNI. Following the example of past efforts to standardize data across ADRCs, SCAN neuroimaging data are integrated with other ADRC data streams within NACC, including the Uniform Data Set (UDS) which includes rich longitudinal demographic, cognitive, and neuropathological data. Current participants from SCAN include individuals from 22 ADRCs between the ages of 50 and 96 who have a cognitive status of cognitively normal (CN), MCI, and dementia. For MCI and dementia patients, more detailed etiological diagnoses included AD dementia (MCI: 67%; dementia: 72%), vascular disease (MCI: 7%; dementia: 2%), and other etiologies (details in Table S1). Participants had ≥ 1 Aβ scan with ^{11}C PiB, FBB, FBP, or [18F]NAV4694 (NAV) and/or tau PET scans (FTP or ^{18}F MK6240). Scans and corresponding metadata are submitted to Laboratory of NeuroImaging (LONI) by each participating ADRC. A contemporaneous structural MRI was not available for many PET scans at the time of this study, so we used the MRI-free PET pipeline to calculate SUVrs. We then converted these B-PIP MRI-free SUVrs to be compatible with SUVrs from B-PIP MRI-dependent pipeline SUVrs using methods described below and in the Supplementary Materials.

2.1.3 | POINTER imaging

Participants from the U.S. POINTER imaging substudy (POINTER Imaging) were recruited from the U.S. POINTER trial, which is testing whether random assignment to either of two multidomain lifestyle interventions (focusing on nutrition, physical exercise, cognitive/social stimulation, health monitoring) that differ in format, intensity, and accountability affects 2-year cognitive change.[6] U.S. POINTER trial participants are between the ages of 60 and 78, lack significant memory impairment, have a global CDR of 0 or 0.5, are sedentary, report a suboptimal diet, and are at risk for future cognitive decline based on family history of memory impairment, race or ethnicity, and/or other risk factors. About 50% of U.S. POINTER trial participants are enrolled into the POINTER imaging substudy and have baseline Aβ (FBB), MRI, and tau PET (MK6240) scans. Individuals with significant memory impairment were excluded, but some individuals may meet criteria for MCI. However, centrally-adjudicated clinical diagnoses for the entire sample are not yet available so all POINTER imaging participants are considered unimpaired for illustration purposes in this study.

RESEARCH IN CONTEXT

1. **Systematic review**: We used PubMed to identify publications examining β-amyloid (Aβ) and tau positron emission tomography (PET) processing streams. There is a need to develop scalable pipelines for rigorous and scalable harmonization of Aβ and tau quantitative outcomes.
2. **Interpretation**: We used the Berkeley PET Imaging Pipeline (B-PIP) to calculate harmonized cross-sectional and longitudinal Aβ and tau measurements using scans from Alzheimer's Disease Neuroimaging Initiative (ADNI) and several other multisite studies and clinical trials.
3. **Future directions**: This manuscript describes the implementation of standardized PET acquisition, analysis, and data sharing methods that were developed in ADNI and are used in other large-scale ADNI. This pipeline facilitates cross-cohort comparisons of large and increasingly heterogenous datasets.

2.1.4 | BACS

The BACS is a longitudinal observational study of normal aging. Participants are CN older adults who were recruited from the local Berkeley community via advertisements and word of mouth. Inclusion criteria for BACS include an mini-mental state exam (MMSE) score ≥ 25, normal daily function, and scores on the California Verbal Learning[7] and Visual Reproduction tests[8] within 1.5 standard deviations of age, sex, and education-adjusted norms. Exclusion criteria include history of neurological disease or substance abuse, cognition-affecting mental illness, or neuroimaging contraindications. Baseline PiB and/or FTP scans were acquired, and longitudinal scans were available for 59% (PiB) and 53% (FTP) of the sample (see Table 1).

2.2 | PET image acquisition and pre-processing

Figure 1 shows a summary of the key harmonization steps described below. Tracer-specific PET image primary acquisition protocols developed by the ADNI, POINTER, and SCAN PET Cores are shown for Aβ PET (Table 2) and tau PET (Table 3).

TABLE 1 Participant demographics and scan characteristics of the study cohorts.

	ADNI	BACS	POINTER imaging	SCAN	All cohorts
Demographics					
Participants (*N*)	1747	253	937	1343	4280
Age (years)	72.9 ± 7.6	75.00 ± 6.6	68.4 ± 5.2	72.3 ± 7.7	71.8 ± 7.4
Sex, % Female	49%	56%	61%	59%	55%
Race, *N*					
White	1454	222	637	971	3284
Black	131	6	135	236	508
Hispanic	76	6	71	66	219
Asian	45	11	30	37	123
Other	41	7	62	31	141
Education (years)	16.3 ± 2.6	17.0 ± 2.1	16.0 ± 2.2	16.4 ± 2.5	16.3 ± 2.5
Global CDR, % 0	43%	–	80%	62%	60%
Clinical Dx % CN	43%	100%	100%*	65%	61%
CN, *N*	748	251	937*	852	2605
MCI, *N*	783	–	–	312	1280
Dementia**, *N*	215	–	–	152	367
APOE-ε4, % carrier	43%	25%	28%	40%	38%
PET					
Amyloid PET					
Tracer	FBB, FBP	PIB	FBB	FBB, FBP, PIB, NAV	FBB, FBP, PIB, NAV
N	377, 1370	253	937	562, 211, 492, 78	1876, 1581, 745, 78
%	22%, 78%	100%	100%	42%, 16%, 37%, 6%	44%, 37%, 17%, 2%
Aβ positive, %	48%	34%	29%	44%	42%
Centiloids	36.1 ± 46.5	15.4 ± 29.5	17.0 ± 25.6	25.1 ± 41.9	27.2 ± 41.1
Scans/participant	2.2 ± 1.3	2.1 ± 1.3	–	–	2.2 ± 1.3
≥ 1 scan (%)	61%	58%	–	–	28%
Follow-up (years)#	2.3 ± 0.8	2.9 ± 1.4	–	–	2.3 ± 0.9
Tracer	FTP	FTP	MK6240	FTP, MK6240	FTP, MK6240
N	925	165	911	289, 266	1388, 1177
%	53%	65%	97%	24%, 21%	32%, 28%
Entorhinal *Z*-score	1.4 ± 2.7	0.7 ± 1.3	0.5 ± 1.9	1.6 ± 3.0	1.1 ± 2.5
MetaROI *Z*-score	1.9 ± 4.3	0.5 ± 1.6	0.2 ± 1.6	1.7 ± 4.2	1.2 ± 3.5
Scans/participant	0.9 ± 1.1	1.2 ± 1.2	–	–	1.0 ± 1.2
≥ 1 scan (%)	26%	34%	–	–	13%
Follow-up (years)#	1.9 ± 1.2	2.3 ± 1.1	–	–	2.0 ± 1.1

Note: All participants are over 50 years of age and have at least one Aβ or one tau scan. Age is calculated as age from baseline amyloid scan.
Abbreviations: APOE, apolipoprotein E; Aβ, amyloid beta; CDR, clinical dementia rating; CN, cognitively normal; FBB, florbetaben; FBP, florbetapir; FTP, [18F]Flortaucipir; MCI, mild cognitive impairment; MetaROI, metatemporal region of interest; N, number; NAV, [18F]NAV4694; PET, positron emission tomography; URG, underrepresented racial and/or ethnic group.
- Not available currently, but will be available in the future.
– Not applicable to the cohort.
Based on participants with ≥ 1 scan.
* Centrally-adjudicated clinical diagnoses are not available for POINTER, but participants lack significant impairment.
**Dementia: ADNI, AD Dementia; SCAN, etiological diagnoses are available in the Supplementary Data.
Missing data.
Race: Total = 5, ADNI = 0, BACS = 1, POINTER = 2, SCAN = 2.
Global CDR: Total = 251, all from BACS.
Diagnosis: Total = 24, all from SCAN.
APOE: Total = 377, ADNI = 177, BACS = 32, POINTER = 51, SCAN = 168.

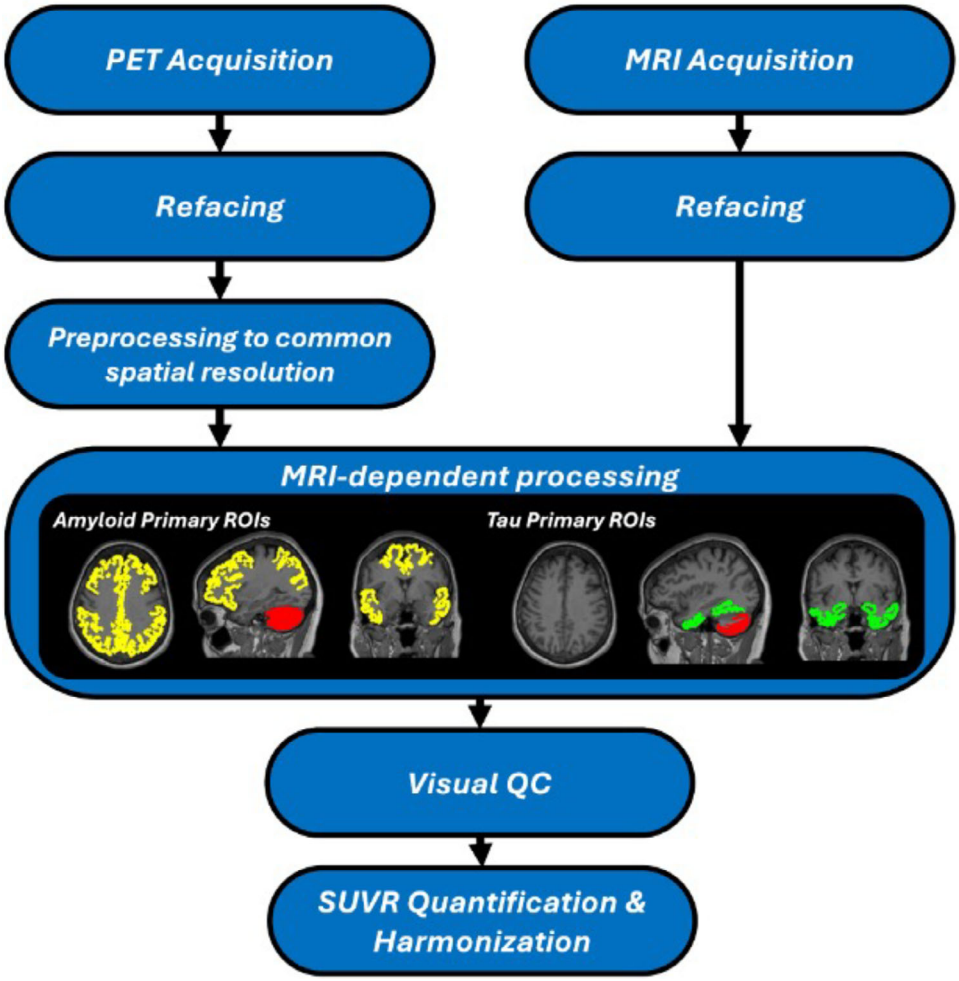

FIGURE 1 PET image processing overview. A summary of the Aβ and tau PET image processing stream is shown. Following tracer-specific Aβ and tau image acquisition and reconstruction, images are defaced (ADNI, SCAN) and pre-processed to adjust for motion and differing scanner resolutions. B-PIP then involves processing a refaced magnetization-prepared rapid gradient echo (MPRAGE) with FreeSurfer to define ROI and reference regions that are sampled from a co-registered PET image, visual QC of the PET co-registered to the FreeSurfer-parcellated anatomical boundaries and MRI, and calculation of SUVrs within tracer-specific ROI described below. Finally, SUVrs are harmonized to account for tracer-related differences, and thresholding is carried out to define positive/abnormal scans. This pipeline is fully automated except for visual QC. A parallel and fully automated MRI-free pipeline and corresponding harmonization information is described below and in the Supplementary Materials. Aβ β-amyloid; ADNI, Alzheimer's Disease Neuroimaging Initiative; B-PIP, Berkeley PET imaging pipeline; MPRAGE, Magnetization-prepared rapid gradient echo; PET, positron emission tomography; QC, quality control; SCAN, standardized centralized Alzheimer's & related dementias neuroimaging; SUVrs, standardized uptake value ratios.

2.2.1 | Initial QC

Attenuation correction is performed using scanner-specific procedures for PET-CT, PET-MRI or PET only scanners, and standard scanner- and site-specific iterative algorithms are employed for image reconstruction. Following PET image acquisition and image upload to the LONI, several QC checks are carried out by the University of Michigan including statistical noise checks, motion assessment across temporal frames, full brain coverage verification, and visual inspections to identify common artifacts.

2.2.2 | Face de-identification

Starting in 2024 with ADNI-4, raw ADNI PET images are "de-faced" by the Mayo Clinic team by replacing facial features in the native space image with an average face, using their automated *mri_reface* software, which was developed and validated using PET scans from ADNI, among others. Visual QC is performed on each scan to ensure complete replacement of the face and non-modification of all brain voxels. This process has a negligible influence on SUVrs, so no transformation is necessary to combine defaced and non-defaced data.[9] A detailed write-up of this process is also available in this issue.[10]

TABLE 2 Aβ PET tracer-specific primary acquisition protocols, thresholds, and CL transformation equations.

Tracer	Cohort	Post-injection acquisition time (min)	Dose ± 10%		Cross-sectional MRI-dependent thresholds (SUVr/CL)	Centiloid transformation equation
			mCi	MBq		
PiB	SCAN, BACS	50–70	15	555	1.21 SUVr 9 CL	CL = 95.57 (MRI-dep SUVr/ CerebGray)−107.04
FBP	ADNI, SCAN, BACS	50–70	10	370	1.11 SUVr 20 CL	CL = 188.22 (MRI-dep SUVr)−189.16
FBB	ADNI, SCAN, POINTER	90–110	8.1	295	1.08 SUVr 18 CL	CL = 157.15 (MRI-dep SUVr)−151.87
NAV	SCAN	50–70	8.1	300	Under development	CL = 109.45 (MRI-dep SUVr)−106.78

Note: CL transformations are all based on whole cerebellum intensity normalization, except MRI-dep PiB, which uses the cerebellar gray matter.
Abbreviations: ADNI, Alzheimer's Disease Neuroimaging Initiative; BACS, Berkeley aging cohort study; CL, Centiloid; FBB, florbetaben; FBP, florbetapir; NAV, [18F]NAV4694; PET, positron emission tomography; PiB, Pittsburgh compound B; SCAN, standardized centralized Alzheimer's & related dementias neuroimaging; SUVrs, standardized uptake value ratios.

TABLE 3 Tau PET tracer-specific acquisition protocols.

Tracer	Cohort	Post-injection acquisition time (min)	Dose ± 10%	
			mCi	MBq
FTP	ADNI, SCAN, BACS	70–105	10	370
MK6240	SCAN, POINTER	90–110	5	185

Note: Tau PET SUVrs are normalized to the inferior cerebellar gray matter.
Abbreviations: ADNI, Alzheimer's disease neuroimaging initiative; BACS, Berkeley aging cohort study; FTP, [18F]Flortaucipir; PET, positron emission tomography; SCAN, standardized centralized Alzheimer's & related dementias neuroimaging; SUVrs, standardized uptake value ratios.

2.2.3 | PET pre-processing

For ADNI, SCAN and POINTER, the Koeppe Lab at University of Michigan carries out pre-processing that results in four sets of "pre-processed" PET images sets in digital imaging and communications in medicine (DICOM) format which are uploaded to LONI. The first two image sets retain the original patient orientation, pixel grid, and intrinsic plane spacing specific to each scanner while the final two image sets are reoriented to a standardized matrix.

1. Co-registered Dynamic: Each 5-min frame in native space (de-faced, when applicable, or original, raw scan) is co-registered to the first extracted frame of the raw image file in order to motion correct the images.
2. Co-registered, Averaged: Individual 5-min frames in the dynamic image set are averaged to produce a single image.
3. Co-reg, Avg, Standardized Image, and Voxel Size: Each tracer type (amyloid and tau separately)'s first scan is reoriented into a standard 160 × 160 × 96 voxel image grid with 1.5 mm^3 voxels using rigid body registration to achieve standard anterior commissure-posterior commissure line (AC-PC) alignment. Subsequent scans are co-registered to their first scan's AC-PC alignment for consistent spatial orientation. Cerebellar gray matter (GM) is used as the reference region for SUVr normalization. Importantly, this initial intensity normalization is later replaced (''divided out'') by tracer-specific reference regions in B-PIP.
4. Co-reg, Avg, Std Img, and Vox Siz, Uniform Resolution: The standardized images are smoothed to a common resolution using scanner-specific 3D-Gaussian filters derived by the University of Michigan team using Hoffman phantom scans carried out at each site.[11] The effective resolution was selected based on the lowest resolution scanners in ADNI, with resolutions initially set to 8 mm^3 full width half maximum (FWHM) and, in 2023, adjusted to 6 mm^3 FWHM to reflect the lowest resolution of the current scanners. In 2023, all Aβ and tau ADNI PET data were re-processed by UC Berkeley retrospectively at 6 mm^3 in order to generate a harmonized dataset at the new resolution. Resulting preprocessed PET DICOMs have a standardized voxel size and spatial resolution.

BACS scans are reconstructed and pre-processed at Berkeley to allow for comparison to preprocessed ADNI data. A 4 mm Gaussian smoothing filter is applied to individual frames during reconstruction, which results in an effective resolution that is comparable to the harmonized 6 mm isotropic resolution achieved in ADNI, POINTER, and SCAN. All preprocessed scans from ADNI, SCAN, POINTER, and BACS are then processed with B-PIP.

2.3 | MRI acquisition and pre-processing

A contemporaneous 3T Magnetization-prepared rapid gradient echo (MPRAGE) (1.5T in BACS) acquired closest in time to each PET scan is used for anatomical definition of PET ROIs in native space. MPRAGE scans are reconstructed locally at sites as overseen by the ADNI Mayo Clinic Rochester team.[12] In ADNI, the MPRAGE was refaced starting in 2024 as described in this issue.[10] Preprocessed, defaced MPRAGEs are downloaded from LONI in DICOM format and converted to neuroimaging informatics technology initiative format using dcm2niix.[13]

Parcellation of native-space regions in the Desikan-Killiany atlas[14] is carried out for each MPRAGE using FreeSurfer v7.1.[15]

2.4 | MRI-dependent B-PIP

Each fully pre-processed PET image is downloaded from LONI (for ADNI, SCAN, and POINTER), co-registered to a contemporaneous MPRAGE using SPM12 (statistical parametric mapping) (see above) and Desikan-Killiany atlas FreeSurfer parcellations are used to calculate mean PET uptake from within tracer-specific primary ROIs and reference regions (see below and Supplementary Materials), as well as all Desikan-Killiany atlas regions.

2.4.1 | Aβ PET

The cortical summary region is made up of frontal, cingulate, parietal, temporal subregions defined by the Desikan-Killiany atlas (see Supplementary Materials for list). Reference regions include whole cerebellum (cerebellar gray for the PiB MRI-dependent pipeline) for cross-sectional analyses and determining Aβ ± status, and for longitudinal analyses, a composite reference region made up of whole cerebellum, brainstem/pons, and eroded subcortical white matter (WM) regions which appears to decrease longitudinal noise.[16–20]

Cortical summary Aβ PET SUVrs are converted to CL using tracer-specific equations derived for B-PIP as described previously[21,22] (see Table 2 and Supplementary Materials for MRI-free pipeline thresholds and conversion equations).

MRI-dependent thresholds for PiB (1.21 / 9CL; cerebellar gray intensity normalization), FBP (1.11/20 CL; whole cerebellum intensity normalization), and FBB (1.08/18 CL; whole cerebellum intensity normalization) are shown in Table 2. These thresholds have been previously validated using several strategies (upper limit of tracer uptake in young controls, Gaussian mixture modeling, and pathology-based validation) as described previously.[21] A previously-validated PiB threshold based on PET distribution volume ratios (DVRs)[23] was converted to the SUVr threshold shown in Table 2 using the best-fit linear relationship between 1039 PiB DVRs and SUVrs from BACS. An MRI-dependent NAV4694 threshold is still under development. Thresholds for use with cortical summary Aβ SUVrs and CLs that are based on the MRI-dependent and MRI-free pipelines are described in the Supplementary Materials.

2.4.2 | Tau PET

Primary ROIs include entorhinal cortex and the temporal metaROI which is made up of bilateral entorhinal, amygdala, parahippocampal, fusiform, inferior temporal, and middle temporal regions as described previously[24] and as defined by the Desikan-Killiany atlas (see Supplementary Materials). An inferior cerebellar GM reference region is created using the native-space, FreeSurfer-defined cerebellar GM with dorsal cerebellum (defined by the reverse-normalized SUIT template) excluded in order to reduce the influence of off-target signal in the dorsal cerebellum.[25] Our primary quantitative outcomes are not corrected for partial volume effects, but as part of B-PIP we carry out partial volume correction (PVC) for all Desikan-Killiany atlas regions, the temporal metaROI, and inferior cerebellar GM reference region using the Geometric Transfer Matrix approach for FTP and MK6240 as previously described[25–27] (see Supplementary Materials). These quantitative outcomes are made available alongside our non-PVC tau data.

Here, we used a *Z*-normalization approach[28] to standardize FTP and MK6240 PET SUVrs from B-PIP, using CN, Aβ-negative individuals age 60–70 years, excluding outliers > 3SD (standard deviation) above the mean, from available cohorts to define the mean and standard deviation used to create *Z*-scores for all available FTP and MK6240 images (Table S2).

2.5 | MRI-free B-PIP

For PET scans without a contemporaneous MRI available, or when our MRI-based pipeline fails visual QC (see below), we use an MRI-free processing approach. Briefly, this process involves spatially normalizing PET images to Aβ and tau PET templates in Montreal Neurological Institute (MNI) space (Figures S1 and S2) and calculating SUVrs for our primary Aβ and tau ROIs.[29] For Aβ, this involves calculation of tracer uptake within the MNI-space GAAIN cortical summary ROI that is used for CL quantification,[22] and for tau, we use an MNI-space atlas described below that parallels the native space Desikan-Killiany atlas used with FreeSurfer. We validated MRI-free SUVrs for each tracer against the gold-standard MRI-dependent B-PIP based on strong associations ($R^2 > 0.90$) between the two measures.

We have developed a novel atlas called the Normalized Probability Desikan-Killiany Atlas (NPDKA) for use in the MRI-free pipeline that is an MNI-space counterpart to the FreeSurfer-based Desikan-Killiany atlas used in our native space, MRI-dependent pipeline.[14] By providing MNI-space regions that parallel the native space, Desikan-Killiany atlas regions generated by FreeSurfer processing, the NPDKA facilitates harmonization of regional Aβ and tau PET measures processed in the MRI-free and MRI-dependent pipelines across multicohort datasets regardless of whether an MPRAGE is consistently available for all scans.

To create the NPDKA, the Freesurfer v7.1 Desikan-Killiany segmentations of 200 CN, Aβ-negative ADNI participants were (1) warped to MNI-152 space using the parameters from their T1 (SPM12 normalize), (2) each ROI mask was smoothed with a 1.5 mm FWHM gaussian kernel to clean the edges, (3) each ROI mask was averaged across the 200 subjects, and (4) voxels within each ROI were normalized to values between 0 and 1 by dividing out the highest voxel probability (see Supplementary Materials and Figure S3). Finally, ROI probability maps were combined into a single whole brain atlas by assigning each voxel to the ROI whose probability map was the highest for that voxel. This allowed us to define atlas-style integer boundaries between ROIs in template space.

Importantly, there are two ways that images processed with the MRI-free pipeline can be used. When all scans in the analysis were processed with the MRI-free pipeline, SUVrs resulting from MRI-free processing can be used without any additional steps. In this case, MRI-free based thresholds (Table S3) can be applied, and Aβ PET SUVrs can be transformed to CLs using the equations in Table S4.

Alternatively, if the majority of the PET images in a dataset were processed with the MRI-dependent pipeline, but some scans cannot be analyzed with that pipeline (due to a missing MRI or failed FreeSurfer segmentation), those scans can be included in the dataset by processing them with the MRI-free pipeline and converting the MRI-free based SUVrs to MRI-dependent "units" using the equations in Table S4 and Figure S4 (Aβ PET, including CL) and Table S5 and Figure S5 (tau PET). This makes the MRI-free-to-MRI-dependent "converted" data compatible with the rest of the MRI-dependent dataset. In this case, MRI-dependent Aβ PET thresholds can be applied to the entire dataset after transformation from MRI-free to MRI-dependent "units."

2.6 | B-PIP visual quality control

We developed a visual QC protocol that involves inspection of a report that is automatically generated for each scan in the MRI-dependent pipeline when processing is complete. This report contains a series of axial slices showing (1) the T1 MRI scan, (2) the FreeSurfer regional parcellation overlaid on the MRI scan, and (3) the FreeSurfer regional parcellation for primary Aβ and tau ROIs and reference regions only overlaid on the MRI-co-registered PET image. Technicians who carry out QC are trained using a standard dataset with common incidental findings that can affect tracer uptake (e.g., meningiomas, small infarcts) and FreeSurfer parcellation and co-registration problems. The visual QC logging process involves flagging instances where the measured values (SUVr or volume) may be unreliable due to anatomical findings or segmentation or registration errors (Figures S6 and S7). FreeSurfer parcellation is re-attempted in order to fix segmentation errors; strategies include a repeat attempt of the original parcellation, or use of additional flags suggested by the FreeSurfer error report. When visual QC results in a partial pass, only primary target and reference regions are provided in the numerical datasets. When visual QC results in a failure after a reprocessing attempt, the MRI-free pipeline can be used for primary ROIs, and MRI-free transformations should be applied prior to merging MRI-free results with the MRI-dependent dataset.

Images are then assigned a quality score based on the assessed reliability:

Full pass (qc_flag = 2): All regions meet reliability criteria

Partial pass (qc_flag = 1): Only the primary target and reference regions are reliable

Fail (qc_flag = 0): The primary target or reference region does not meet reliability standards

Visual QC results are provided in UC Berkeley datasets analyzed with the MRI-dependent pipeline so that users can choose to avoid potential sources of measurement error that could confound the analyses. A total of 54 scans from ADNI, BACS, and POINTER have partial pass or fail results; after reprocessing attempts, there were a total of 4 fails and 48 partial pass results (Table S6). Visual QC results are not provided with MRI-free datasets (e.g., SCAN), since we have not observed failures with this pipeline based on visual QC of 1000 MRI-free processed images from SCAN (unpublished data).

More details and example Visual QC images are provided in the Supplementary Materials.

2.7 | Available quantitative PET datasets analyzed with B-PIP

B-PIP generates quantitative PET outcomes in spreadsheet format (with accompanying data dictionaries and methods documents) for each Desikan-Killiany atlas region as well as tracer-specific composite ROIs, reference regions, and Aβ thresholds as described above and shown in Table 2. Our primary pipeline for most numerical datasets is MRI-dependent, except for SCAN, where the current primary pipeline is MRI-free. An MRI-free dataset can be used in an analysis without any further transformations when all PET images were analyzed with the MRI-free pipeline. For datasets or analyses that combine MRI-free and MRI-dependent based SUVrs (for example, in cases missing an MRI or with failed visual QC due to problems with FreeSurfer segmentation), MRI-free based SUVrs can be converted to MRI-dependent "units" in order to make these outcomes compatible (see Section 2.5 and Tables S4 and S5).

Spreadsheets with these numerical regional quantitative PET data, corresponding regional volumes, visual QC results as well as data dictionaries and documents summarizing the overall pipeline and any study-specific methods can be downloaded from LONI (ADNI, POINTER imaging) or accessed via the National Alzheimer's Coordinating Center (SCAN) or through a data request (BACS). Each study has specific data request procedures that involve data use agreements and/or study proposal review.

3 | RESULTS

3.1 | Overview of ADNI, SCAN, POINTER imaging, and BACS participants

We analyzed 6659 Aβ and 3446 tau PET scans from 4280 participants across all four cohorts using B-PIP as outlined in Figure 1 and described above. Demographic characteristics were highly variable across cohorts (Table 1), but overall the participants included in this study had a mean age of 71.8 ± 7.4, 55% were female and 23% of individuals were from under-represented racial groups.A total of = 61% of the overall sample was cognitively unimpaired and the remaining 39% included individuals with MCI or dementia. Of patients from SCAN at a clinical stage of MCI or AD clinical stage, 31% had a non-AD clinical diagnosis. For Aβ PET, there were similar proportions of participants

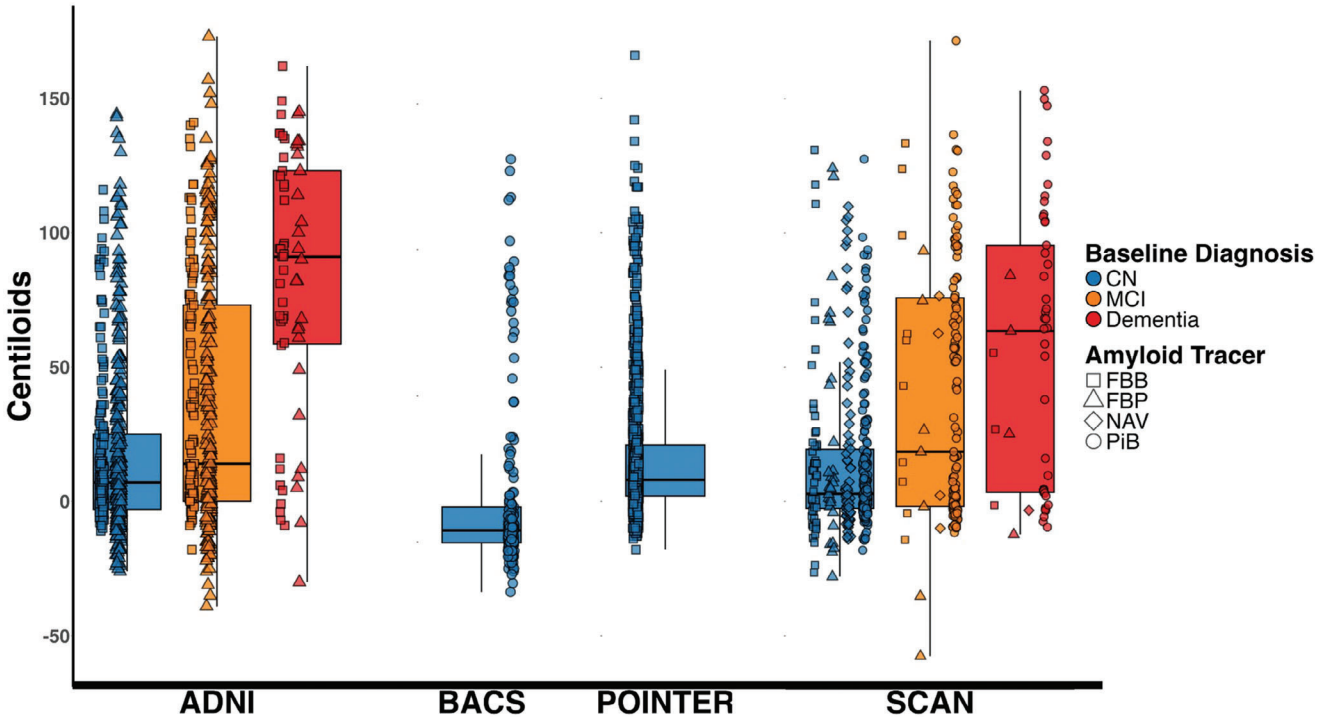

FIGURE 2 CL measurements for 4280 baseline scans processed with B-PIP and harmonized across Aβ tracers and cohort. CL values are shown for each participant's baseline Aβ scan by cohort and clinical diagnosis. CL are normalized to the whole cerebellum (except PiB, which uses cerebellar gray matter intensity normalization for the MRI-dependent pipeline only). Each shape represents a different amyloid tracer. Aβ, β-amyloid; AD, Alzheimer's disease; B-PIP, Berkeley PET imaging pipeline; CL, Centiloid; CN, cognitively normal; FBB, florbetaben; FBP, florbetapir; MCI, mild cognitive impairment; MRI, magnetic resonance imaging; PET, positron emission tomography; PiB, Pittsburgh compound B.

with FBB (44%) and FBP (37%), and smaller proportions with PIB (17%) and NAV (2%). A total of 28% of the overall Aβ PET sample had longitudinal Aβ PET scans (all from ADNI or BACs) over 2.3 ± 0.9 years. For tau PET, there were similar proportions of participants who had FTP (54%) and MK6240 (46%), and 13% of the overall tau PET sample had longitudinal tau PET scans (all with FTP, from ADNI or BACs) over 2.0 ± 1.1 years.

3.2 | Aβ PET

Aβ PET Cortical Summary data for 4280 baseline scans are shown in CL across all cohorts, separated by patient diagnosis and tracer (Figure 2). The cohorts include differing proportions of individuals across diagnostic groups, so cross-cohort interpretation of CL differences is not meaningful, but the distribution of CLs is visually similar for FBP, FBB, and NAV across the cohorts. Notably, SCAN SUVrs were calculated using the MRI-free pipeline and converted to CLs using equations based on the MRI-free quantification, whereas SUVrs for the other cohorts were calculated using CL equations based on MRI-dependent quantification. The distribution of CLs across all cohorts demonstrates that conversion of SUVrs from this image analysis pipeline to CLs can be carried out successfully across a variety of acquisition protocols and tracers.

3.3 | Tau PET

Baseline *Z*-transformed entorhinal cortex (Figure 3A) and the temporal metaROI (Figure 3B) tau PET data are shown for 2565 baseline scans, separated by Aβ PET across all cohorts for FTP and MK6240. SCAN tau PET SUVrs were calculated using the MRI-free pipeline and converted to MRI-dependent SUVrs before *Z*-scoring, whereas tau PET SUVrs for the other cohorts were calculated using the MRI-dependent pipeline and converted directly to *Z* scores. This allowed us to use the same reference sample data for all *Z*-scores regardless of processing approach. Because each cohort has differing proportions of individuals within diagnostic groups, cross-cohort interpretation of *Z*-normalized tau PET data is not meaningful, but entorhinal and temporal tau are consistently higher for Aβ PET+ individuals across all cohorts and diagnostic groups.

3.4 | Longitudinal Aβ and tau PET

Longitudinal Aβ CLs (Figure 4A) and longitudinal entorhinal tau *Z*-scored FTP (Figure 4B) and temporal metaROI *Z*-scored FTP (Figure 4C) PET trajectories are shown for studies with available longitudinal data (ADNI and BACS). For participants with longitudinal data, mean Aβs PET follow-up time was 2.2 ± 0.8 years for ADNI

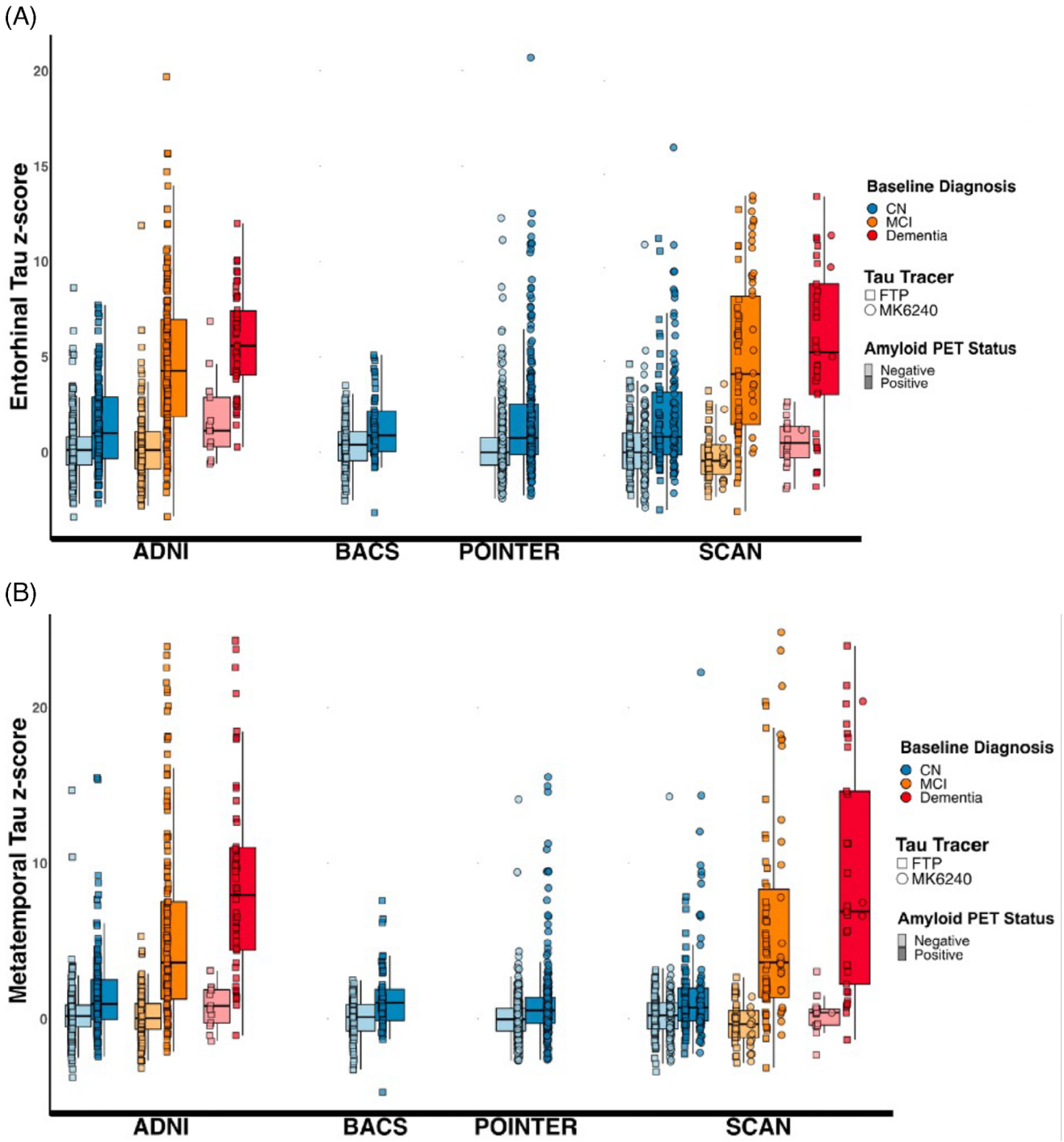

FIGURE 3 Tau PET measurements for 2565 baseline scans processed with B-PIP and harmonized across tau tracers and studies. *Z*-scored (A) entorhinal cortex tau and (B) temporal metaROI tau is shown by study, A$\beta \pm$ status and diagnosis. *Z* scores were calculated using tracer-specific samples of amyloid-negative, < 70 years old, CN individuals used to calculate mean and standard deviation values (see Table S1). The light shade of each color represents Aβ- individuals, and the darker shade represents Aβ+ individuals. Each shape represents a different tau tracer. Tau SUVrs to derive the *Z*-scores are normalized to the inferior cerebellar gray matter. Aβ, β-amyloid; AD, Alzheimer's disease; B-PIP, Berkeley PET imaging pipeline; CN, cognitively normal; FTP, [18F]Flortaucipir; MCI, mild cognitive impairment; PET, positron emission tomography; ROI, region of interest; SUVrs, standardized uptake value ratios.

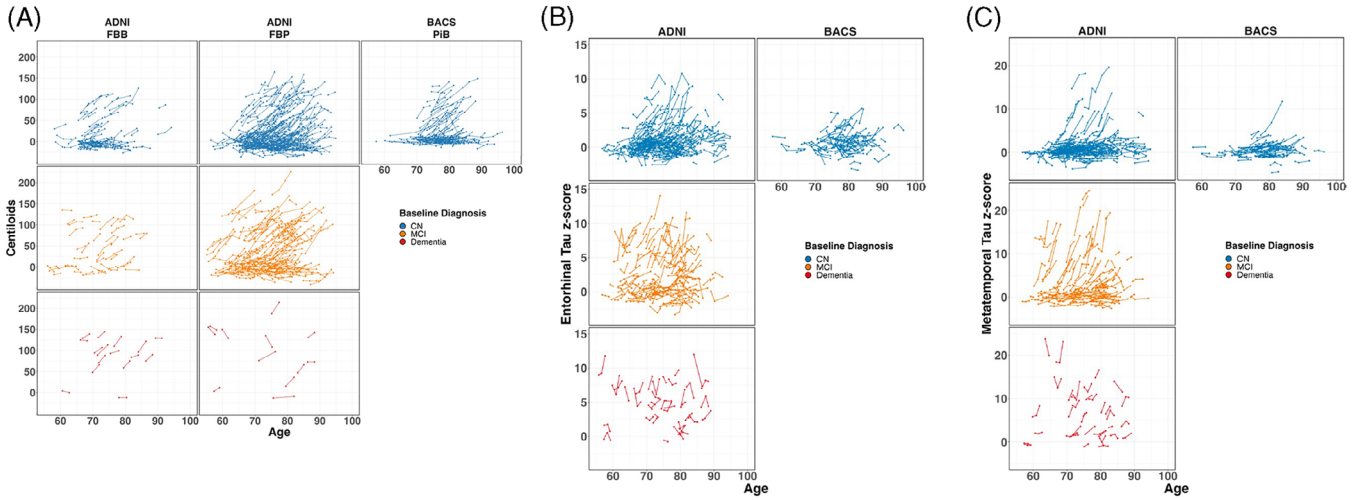

FIGURE 4 Longitudinal Aβ and tau PET trajectories. (A) Longitudinal CLs by diagnosis, tracer and study. CLs are normalized to the composite reference region, except PiB, which uses the cerebellar gray matter region. Each shape represents a different amyloid tracer. *Z*-scores for longitudinal (B) entorhinal cortex and (C) temporal tau are shown by diagnosis and study. Tau SUVrs to derive the *Z*-scores are normalized to the inferior cerebellar gray matter. Only longitudinal FTP data were available for ADNI and BACS at the time of this study. One participant from ADNI with dementia who had a temporal metaROI *Z*-score of 41 is not shown. Aβ, β-amyloid; AD, Alzheimer's disease; ADNI, Alzheimer's Disease Neuroimaging Initiative; BACS, Berkeley aging cohort study; CL, Centiloid; CN, cognitively normal; FBB, florbetaben; FBP, florbetapir; FTP, [18F]Flortaucipir; MCI, mild cognitive impairment; PET, positron emission tomography; PIB, Pittsburgh compound B; PiB, Pittsburgh compound B; SUVrs, standardized uptake value ratios.

and 2.9+/1.4 years for BACs, with a maximum Aβ follow-up of 8.1 years and six scans (ADNI); and the mean tau PET follow-up time was 1.9 ± 1.2 years for ADNI and 2.3 ± 1.1 years for BACs, with a maximum tau follow-up of 5.9 years and six scans (ADNI). Similar to the cross-sectional data, SCAN PET SUVrs were calculated using the MRI-free pipeline and converted to harmonized units (CL for Aβ and *Z*-scores for tau), whereas PET SUVrs for the other cohorts were calculated using the MRI-dependent pipeline and converted to harmonized units.

4 | DISCUSSION

Detection of in vivo Aβ and tau with PET imaging has played an increasingly important role in large-scale observational studies, clinical trials, and in the clinic. However, interpretation of image data outcomes is complicated by the use of multiple scanners, tracers, and image processing approaches, all of which influence measurements of tracer uptake.[30] As a result, quantitative outcomes of PET scans that are acquired and processed in different studies cannot be merged or directly compared, limiting the potential of rigorous multicohort analyses. To overcome these challenges, we have developed a scalable pipeline (B-PIP) for harmonized, multisite image acquisition and analysis. B-PIP is designed for rigorous quantification of multiple Aβ and tau tracers from within anatomically-defined regions in native space as well as tracer-specific composite and reference regions. It also has features to flexibly accommodate other situations such as the lack of an available structural MRI. Finally, the pipeline includes pipeline- and tracer-specific Aβ positivity thresholds and CL conversion equations, can be adapted for use with emerging tau standardization approaches and is fully automated except for a visual quality assurance step. Harmonized quantitative outcomes and corresponding cohort-specific methods documents are available in spreadsheets for use by the scientific community. The results described here demonstrate the feasibility of implementing B-PIP across multicohort PET datasets by illustrating harmonized outcomes from 6659 Aβ scans (including up to 8 years of longitudinal follow-up in ADNI) and 3446 tau PET scans (including almost 6 years of longitudinal tau in ADNI) for a total of 10,105 scans from 4280 participants across the disease spectrum.

The PET Core has addressed a number of harmonization challenges over different phases of ADNI including varying scanner image resolutions,[11] harmonization of multiple Aβ and tau tracers with variable characteristics,[31] out-of-sample validation of positivity thresholds,[21] atlas-based definition of ROI with or without an MRI,[29] and visual inspection of co-registration and regional segmentation results as described here. We have also incorporated updates to the pipeline that have led to periodic re-analysis of the entire ADNI PET dataset, due to new software (e.g., updated FreeSurfer versions), and improvements in scanner resolution resulting in a change from 8 to 6 mm common spatial resolution. Together, the harmonization strategies developed in response to these challenges comprise the PET image preprocessing and B-PIP described here, leading to harmonized multicohort outcomes that are directly comparable across studies (Figures 2–4). These outcomes are updated regularly as scans become available, and spreadsheets are shared alongside cohort-specific methods documents with the scientific community. This pipeline has also been implemented by our team in related studies not described here, including the ADNI Late Life Depression study,[32] the ADNI Vietnam War Veterans study,[33] the Head-to-Head Harmonization of Tau

Tracers in Alzheimer's Disease (HEAD) study,[34] the Metformin in Alzheimer's Dementia Prevention (MAP) trial,[35] and the 4 Repeat Tauopathy Neuroimaging Initiative (4RTNI),[36] and could be broadly applicable to other existing datasets and future studies and trials in which PET image acquisition protocols are compatible.

Several other MRI-free image processing pipelines have been developed that share some features with B-PIP.[37] Computation analysis of PET by the Australian Imaging Biomarker Lifestyle study (CapAIBL) is an MRI-free quantification approach that has been implemented across studies,[38] and includes tracer-specific CL transformations.[39] The robust PET-Only Processing (rPOP) pipeline for Aβ quantification has been validated in several large datasets such as Imaging Dementia—Evidence for Amyloid Scanning (IDEAS) and ADNI, with code that is publicly available.[40] Amyloid IQ[41] and tau IQ[42] are automated processes for quantification that account for regional variability in tracer-specific binding patterns, including off-target binding. These pipelines involve PET-only spatial normalization and calculation of regional tracer uptake in template space regions applied at the group level, which share methodological features with our MRI-free pipeline (Supplementary Materials).

There are advantages and disadvantages to MRI-free processing. MRI-free processing is a flexible analysis approach in that it can either be used as a primary analysis approach, when the entire dataset was processed with this pipeline, or it can be used for a subset of data (when MRIs are not available or anatomical definition based on the MRI fails). In the latter case, MRI-free-based SUVrs can be transformed to be compatible with the rest of the MRI-dependent dataset using the conversion equations defined in the Supplementary Materials. Despite these advantages, the MRI-based pipeline is the primary B-PIP approach because of its use of individual anatomy to sample PET tracer uptake. The MRI-based pipeline relies on a co-registered MRI to define ROIs in native space, and for each scan acquired longitudinally, leading to image sampling that is sensitive to morphological characteristics that differ from individual to individual, and from scan to scan over time within each individual. In addition, native space definition of ROI optimizes separation of on-target tracer uptake in ROI versus off-target uptake that can occur in neighboring regions. Influences of off-target signal may be greater when images are warped into template space, blurring boundaries between GM and regions that are vulnerable to off-target signal including WM, cerebrospinal fluid, meninges and bone.[26,43]

While the use of CLs is well established for standardization of Aβ PET outcomes across tracers, tau standardization is still an ongoing area of research that involves unique challenges that complicate direct application of the CL approach used for Aβ PET. Tau accumulation follows a regionally-specific pattern of progression[44]; the regions we included in this study are areas of frequent accumulation in normal aging (entorhinal cortex) and AD (temporal metaROI), but other AD-specific temporal regions have been identified.[45] In addition, regional patterns of tau burden and accumulation are also variable across individuals[46] and dependent on disease stage and clinical diagnosis, as well vulnerability to tracer-specific off-target binding patterns, complicating selection of a fixed region for standardization. In this study, we presented FTP and MK6240 tau PET data harmonized using a *Z*-normalization approach. Several other approaches have been proposed including converting tau PET SUVrs to a CL-like scale,[47,48] but there is currently limited data comparing different tracers in the same individuals. A tau PET tracer head-to-head study designed to generate standardization approaches for FTP, MK6240, and PI2620 is underway.[34] Finally, partial-volume corrected (PVC) tau PET data are not shown here, but PVC using the Geometric Transfer Matrix approach has been developed and validated for FTP and MK6240 in our lab (see Supplementary Materials)[25,26] and is available in parallel with non-PVC tau PET data.

This work has several strengths and limitations. Strengths include the application of a uniform approach to several large cohorts of unimpaired and impaired individuals, demonstrating the feasibility for applying harmonized methods across future multisite and multitracer PET datasets. This increases accessibility to the AD research community, particularly for scientists who are not directly involved in the studies. Large sample sizes are likely to increase generalizability of findings, the representativeness of individuals included in these samples is another critical factor that influences generalizability. Participants included in the cohorts presented here have varying degrees of racial and ethnic diversity; BACS participants lack geographical and racial and ethnic diversity, ADNI participants are geographically diverse but lack racial and ethnic diversity, although enrollment of individuals from under-represented racial and ethnic groups is a key goal of ADNI4. POINTER participants have relatively greater geographical, racial, and ethnic diversity, and diversity is highly variable across ADRC sites contributing data to SCAN. Limitations include data storage requirements and data tracking challenges related to curating and tracking large complex image datasets.

5 | CONCLUSION

B-PIP is a scalable image processing stream that is the product of a collaborative effort across ADNI investigators over two decades to minimize variability in quantitative PET measurements related to multisite and multitracer imaging.[1] This pipeline has been used to harmonize measurements from thousands of Aβ and tau PET scans acquired in ADNI as well as other multisite studies and trials, and these measurements have been made available to the scientific community. The methods used for acquisition, analysis, and data sharing developed in ADNI can be adapted for use in other datasets and future AD neuroimaging studies, facilitating cross-cohort comparisons of large and increasingly heterogenous datasets.

ACKNOWLEDGMENTS

We thank all ADNI, POINTER, BACS, and SCAN leadership, participants, and site staff for their contributions to data collection. We thank ADNI, POINTER, BACS, SCAN, and LONI staff for their help with to image data acquisition oversight, tracking, and processing, including Leslie Gordineer, Karen Crawford, Virginia Roberts, Brett Borowski, Matthew Senjem, and Ashritha Reddy. ADNI: Data

collection and sharing for this project was funded by the Alzheimer's Disease Neuroimaging Initiative (ADNI) (National Institutes of Health Grant U01 AG024904). ADNI is funded by the National Institute on Aging, the National Institute of Biomedical Imaging and Bioengineering, and through generous contributions from the following: Alzheimer's Association; Alzheimer's Drug Discovery Foundation; Araclon Biotech; BioClinica, Inc.; Biogen Idec Inc.; Bristol-Myers Squibb Company; Eisai Inc.; Elan Pharmaceuticals, Inc.; Eli Lilly and Company; EuroImmun; F. Hoffmann-La Roche Ltd and its affiliated company Genentech, Inc.; Fujirebio; GE Healthcare;; IXICO Ltd.; Janssen Alzheimer Immunotherapy Research & Development, LLC.; Johnson & Johnson Pharmaceutical Research & Development LLC.; Medpace, Inc.; Merck & Co., Inc.; Meso Scale Diagnostics, LLC.; NeuroRx Research; Neurotrack Technologies; Novartis Pharmaceuticals Corporation; Pfizer Inc.; Piramal Imaging; Servier; Synarc Inc.; and Takeda Pharmaceutical Company. The Canadian Institutes of Rev December 5, 2013 Health Research is providing funds to support ADNI clinical sites in Canada. Private sector contributions are facilitated by the Foundation for the National Institutes of Health (www.fnih.org). The grantee organization is the Northern California Institute for Research and Education, and the study is coordinated by the Alzheimer's Disease Cooperative Study at the University of California, San Diego. ADNI data are disseminated by the Laboratory for NeuroImaging at the University of Southern California. This work was also supported in part by the Intramural Research Program of the National Institute on Aging (NIA), and the Center for Alzheimer's and Related Dementias (CARD), within the Intramural Research Program of the NIA and the National Institute of Neurological Disorders and Stroke (AG000546). **POINTER imaging**: This study is supported by the National Institutes of Health (R01AG062689) and the Alzheimer's Association (U.S. POINTER-19-611541). **SCAN**: The NACC database is funded by NIA/NIH Grant U24 AG072122. SCAN is a multi-institutional project that was funded as a U24 grant (AG067418) by the National Institute on Aging in May 2020. Data collected by SCAN and shared by NACC are contributed by the NIA-funded ADRCs as follows: Arizona Alzheimer's Center—P30 AG072980 (PI: Eric Reiman, MD); R01 AG069453 (PI: Eric Reiman (contact), MD); P30 AG019610 (PI: Eric Reiman, MD); and the State of Arizona which provided additional funding supporting our center; Boston University—P30 AG013846 (PI Neil Kowall MD); Cleveland ADRC—P30 AG062428 (James Leverenz, MD); Cleveland Clinic, Las Vegas – P20AG068053; Columbia—P50 AG008702 (PI Scott Small MD); Duke/UNC ADRC – P30 AG072958; Emory University—P30AG066511 (PI Levey Allan, MD, PhD); Indiana University—R01 AG19771 (PI Andrew Saykin, PsyD); P30 AG10133 (PI Andrew Saykin, PsyD); P30 AG072976 (PI Andrew Saykin, PsyD); R01 AG061788 (PI Shannon Risacher, PhD); R01 AG053993 (PI Yu-Chien Wu, MD, PhD); U01 AG057195 (PI Liana Apostolova, MD); U19 AG063911 (PI Bradley Boeve, MD); and the Indiana University Department of Radiology and Imaging Sciences; Johns Hopkins—P30 AG066507 (PI Marilyn Albert, Phd.); Mayo Clinic—P50 AG016574 (PI Ronald Petersen MD PhD); Mount Sinai—P30 AG066514 (PI Mary Sano, PhD); R01 AG054110 (PI Trey Hedden, PhD); R01 AG053509 (PI Trey Hedden, PhD); New York University—P30AG066512-01S2 (PI Thomas Wisniewski, MD); R01AG056031 (PI Ricardo Osorio, MD); R01AG056531 (PIs Ricardo Osorio, MD; Girardin Jean-Louis, PhD); Northwestern University—P30 AG013854 (PI Robert Vassar PhD); R01 AG045571 (PI Emily Rogalski, PhD); R56 AG045571, (PI Emily Rogalski, PhD); R01 AG067781, (PI Emily Rogalski, PhD); U19 AG073153, (PI Emily Rogalski, PhD); R01 DC008552, (M.-Marsel Mesulam, MD); R01 AG077444, (PIs M.-Marsel Mesulam, MD, Emily Rogalski, PhD); R01 NS075075 (PI Emily Rogalski, PhD); R01 AG056258 (PI Emily Rogalski, PhD); Oregon Health and Science University—P30 AG008017 (PI Jeffrey Kaye MD); R56 AG074321 (PI Jeffrey Kaye, MD); Rush University—P30 AG010161 (PI David Bennett MD); Stanford – P30AG066515; P50 AG047366 (PI Victor Henderson MD MS); University of Alabama, Birmingham – P20; University of California, Davis—P30 AG10129 (PI Charles DeCarli, MD); P30 AG072972 (PI Charles DeCarli, MD); University of California, Irvine—P50 AG016573 (PI Frank LaFerla PhD); University of California, San Diego—P30AG062429 (PI James Brewer, MD, PhD); University of California, San Francisco—P30 AG062422 (Rabinovici, Gil D., MD); University of Kansas—P30 AG035982 (Russell Swerdlow, MD); University of Kentucky—P30 AG028283-15S1 (PIs Linda Van Eldik, PhD and Brian Gold, PhD); University of Michigan ADRC—P30AG053760 (PI Henry Paulson, MD, PhD) P30AG072931 (PI Henry Paulson, MD, PhD) Cure Alzheimer's Fund 200775 - (PI Henry Paulson, MD, PhD) U19 NS120384 (PI Charles DeCarli, MD, University of Michigan Site PI Henry Paulson, MD, PhD) R01 AG068338 (MPI Bruno Giordani, PhD, Carol Persad, PhD, Yi Murphey, PhD) S10OD026738-01 (PI Douglas Noll, PhD) R01 AG058724 (PI Benjamin Hampstead, PhD) R35 AG072262 (PI Benjamin Hampstead, PhD) W81XWH2110743 (PI Benjamin Hampstead, PhD) R01 AG073235 (PI Nancy Chiaravalloti, University of Michigan Site PI Benjamin Hampstead, PhD) 1I01RX001534 (PI Benjamin Hampstead, PhD) IRX001381 (PI Benjamin Hampstead, PhD); University of New Mexico—P20 AG068077 (Gary Rosenberg, MD); University of Pennsylvania—State of PA project 2019NF4100087335 (PI David Wolk, MD); Rooney Family Research Fund (PI David Wolk, MD); R01 AG055005 (PI David Wolk, MD); University of Pittsburgh—P50 AG005133 (PI Oscar Lopez MD); University of Southern California—P50 AG005142 (PI Helena Chui MD); University of Washington—P50 AG005136 (PI Thomas Grabowski MD); University of Wisconsin—P50 AG033514 (PI Sanjay Asthana MD FRCP); Vanderbilt University – P20 AG068082; Wake Forest—P30AG072947 (PI Suzanne Craft, PhD); Washington University, St. Louis—P01 AG03991 (PI John Morris MD); P01 AG026276 (PI John Morris MD); P20 MH071616 (PI Dan Marcus); P30 AG066444 (PI John Morris MD); P30 NS098577 (PI Dan Marcus); R01 AG021910 (PI Randy Buckner); R01 AG043434 (PI Catherine Roe); R01 EB009352 (PI Dan Marcus); UL1 TR000448 (PI Brad Evanoff); U24 RR021382 (PI Bruce Rosen); Avid Radiopharmaceuticals / Eli Lilly; Yale—P50 AG047270 (PI Stephen Strittmatter MD PhD); R01AG052560 (MPI: Christopher van Dyck, MD; Richard Carson, PhD); R01AG062276 (PI: Christopher van Dyck, MD); 1Florida—P30AG066506-03 (PI Glenn Smith, PhD); P50 AG047266 (PI Todd Golde MD PhD). **BACS**: This study is supported by the National Institutes of Health (R01AG062542).

CONFLICT OF INTEREST STATEMENT

Susan M. Landau is on the DSMB for KeifeRX and the NIH IPAT study and has received speaking honoraria from Eisai and IMPACT-AD. S.L. Baker has served as a consultant for Genentech. William J. Jagust has served as a consultant to Biogen, Novartis, Lilly, and Clario. JiaQie Lee, Jacinda Taggett, Trevor Chadwick, Alice Murphy, Tyler J. Ward, Charles DeCarli, Theresa M. Harrison, Clifford R. Jack, Christopher G. Schwarz, Prashanthi Vemuri, Martin S. Boswell, and Robert A. Koeppe have no conflicts of interest. Author disclosures are available in the Supporting Information.

DATA AVAILABILITY STATEMENT

All ADNI data presented in this manuscript are available to the scientific community at the ADNI data repository at the Laboratory of Neuroimaging (http://adni.loni.usc.edu.). SCAN data is available through the National Alzheimer's Coordinating Center (NACC) (http://scan.naccdata.org). POINTER imaging data is available through data requests (uspointer.net) and LONI, and will be available in the future on the Global Alzheimer's Association Interactive Network (GAAIN). BACS data are available via a data request (https://jagustlab.neuro.berkeley.edu).

CONSENT STATEMENT

Participants in all studies gave informed consent through their local IRBs prior to study participation.

REFERENCES

1. Jagust WJ, Koeppe RA, Rabinovici GD, Villemagne VL, Harrison TM, Landau SM. Alzheimer's Disease Neuroimaging Initiative. The ADNI PET Core at 20. *Alzheimers Dement*. 2024;20(10):7340-7349. doi:10.1002/alz.14165
2. Mormino EC, Kluth JT, Madison CM, et al. Episodic memory loss is related to hippocampal-mediated beta-amyloid deposition in elderly subjects. *Brain*. 2009;132(Pt 5):1310-1323. doi:10.1093/brain/awn320
3. Weiner MW, Veitch DP, Aisen PS, et al. The Alzheimer's disease neuroimaging initiative 3: continued innovation for clinical trial improvement. *Alzheimers Dement*. 2017;13(5):561-571. doi:10.1016/j.jalz.2016.10.006
4. Petersen RC, Aisen PS, Beckett LA, et al. Alzheimer's disease neuroimaging initiative (ADNI): clinical characterization. *Neurology*. 2010;74(3):201-209. doi:10.1212/WNL.0b013e3181cb3e25
5. Standardized Centralized Alzheimer's & Related Dementias Neuroimaging (SCAN). The University of Arizona Health Sciences; 2019. https://scan.naccdata.org/
6. Baker LD, Snyder HM, Espeland MA, et al. Study design and methods: U.S. study to protect brain health through lifestyle intervention to reduce risk (U.S. POINTER). *Alzheimers Dement*. 2024;20(2):769-782. doi:10.1002/alz.13365
7. Delis D. California Verbal Learning Test. 2nd ed. The Psychological Corporation; 2000
8. Wechsler D. Wechsler Adult Intelligence Scale-Revised; 1981
9. Schwarz CG, Kremers WK, Lowe VJ, et al. Face recognition from research brain PET: an unexpected PET problem. *Neuroimage*. 2022;258:119357. doi:10.1016/j.neuroimage.2022.119357
10. Schwarz CG, Choe M, Rossi S, et al. Implementation and validation of face de-identification (de-facing) in ADNI-4. *Alzheimers Dement*. 2022;258:119357
11. Joshi A, Koeppe RA, Fessler JA. Reducing between scanner differences in multi-center PET studies. Multicenter study research support, N.I.H., extramural. *Neuroimage*. 2009;46(1):154-159. doi:10.1016/j.neuroimage.2009.01.057
12. Jack CR, Arani A, Borowski B, et al. Overview of ADNI MRI. *Alzheimers Dement*. 2024;20(10):7350-7360. doi:10.1002/alz.14166
13. Rorden C. https://github.com/rordenlab/dcm2niix
14. Desikan RS, Ségonne F, Fischl B, et al. An automated labeling system for subdividing the human cerebral cortex on MRI scans into gyral based regions of interest. *Neuroimage*. 2006;31(3):968-980. doi:S1053-8119(06)00043-7
15. FreeSurfer. surfer.nmr.mgh.harvard.edu
16. Koeppe RA. Data analysis for amyloid PET imaging: longitudinal studies. Paper presented at: Human Amyloid Imaging; 2013; Miami, FL
17. Brendel M, Hogenauer M, Delker A, et al. Improved longitudinal [(18)F]-AV45 amyloid PET by white matter reference and VOI-based partial volume effect correction. *Neuroimage*. 2015;108:450-459. doi:10.1016/j.neuroimage.2014.11.055
18. Chen K, Roontiva A, Thiyyagura P, et al. Improved power for characterizing longitudinal amyloid-beta PET changes and evaluating amyloid-modifying treatments with a cerebral white matter reference region. *J Nucl Med*. 2015;56(4):560-566. doi:10.2967/jnumed.114.149732
19. Landau SM, Fero A, Baker SL, et al. Measurement of longitudinal beta-amyloid change with 18F-florbetapir PET and standardized uptake value ratios. *J Nucl Med*. 2015;56(4):567-574. doi:10.2967/jnumed.114.148981
20. Schwarz CG, Senjem ML, Gunter JL, et al. Optimizing PiB-PET SUVR change-over-time measurement by a large-scale analysis of longitudinal reliability, plausibility, separability, and correlation with MMSE. *Neuroimage*. 2017;144(Pt A):113-127. doi:10.1016/j.neuroimage.2016.08.056
21. Royse SK, Minhas DS, Lopresti BJ, et al. Validation of amyloid PET positivity thresholds in centiloids: a multisite PET study approach. *Alzheimers Res Ther*. 2021;13(1):1-10
22. Klunk WE, Koeppe RA, Price JC, et al. The Centiloid project: standardizing quantitative amyloid plaque estimation by PET. *Alzheimers Dement*. 2015;11(1):1-15. doi:10.1016/j.jalz.2014.07.003
23. Villeneuve S, Rabinovici GD, Cohn-Sheehy BI, et al. Existing Pittsburgh compound-B positron emission tomography thresholds are too high: statistical and pathological evaluation. *Brain*. 2015;138(Pt 7):2020-2033. doi:10.1093/brain/awv112
24. Jack CR, Jr., Wiste HJ, Weigand SD, et al. Defining imaging biomarker cut points for brain aging and Alzheimer's disease. *Alzheimers Dement*. 2017;13(3):205-216. doi:10.1016/j.jalz.2016.08.005
25. Baker SL, Maass A, Jagust WJ. Considerations and code for partial volume correcting [(18)F]-AV-1451 tau PET data. *Data Brief*. 2017;15:648-657. doi:10.1016/j.dib.2017.10.024
26. Harrison TM, Ward TJ, Murphy A, et al. Optimizing quantification of MK6240 tau PET in unimpaired older adults. *Neuroimage*. 2023;265:119761
27. Rousset OG, Ma Y, Evans AC. Correction for partial volume effects in PET: principle and validation. *J Nucl Med*. 1998;39(5):904-911
28. Vemuri P, Lowe VJ, Knopman DS, et al. Tau-PET uptake: regional variation in average SUVR and impact of amyloid deposition. *Alzheimers Dement*. 2017;6:21-30. doi:10.1016/j.dadm.2016.12.010
29. Landau SM, Ward TJ, Murphy A, et al. Quantification of amyloid beta and tau PET without a structural MRI. *Alzheimers Dement*. 2022;19(2):444-455
30. Bollack A, Pemberton HG, Collij LE, et al. Longitudinal amyloid and tau PET imaging in Alzheimer's disease: a systematic review of methodologies and factors affecting quantification. *Alzheimers Dement*. 2023;19(11):5232-5252. doi:10.1002/alz.13158
31. Landau SM, Breault C, Joshi AD, et al. Amyloid-beta imaging with Pittsburgh compound B and florbetapir: comparing radiotracers and quantification methods. Comparative study research support, N.I.H.,

extramural research support, non-U.S. Gov't. *J Nucl Med*. 2013;54(1):70-77. doi:10.2967/jnumed.112.109009
32. Mackin RS, Insel PS, Landau S, et al. Late-life depression is associated with reduced cortical amyloid burden: findings from the Alzheimer's disease neuroimaging initiative depression project. *Biol Psychiatry*. 2021;89(8):757-765
33. Weiner MW, Harvey D, Hayes J, et al. Effects of traumatic brain injury and posttraumatic stress disorder on development of Alzheimer's disease in Vietnam Veterans using the Alzheimer's disease neuroimaging initiative: preliminary report. *Alzheimers Dement*. 2017;3(2):177-188. doi:10.1016/j.trci.2017.02.005
34. Head-to-head harmonization of tau tracers in Alzheimer's disease (HEAD). https://clinicaltrials.gov/study/NCT05361382
35. Metformin in Alzheimer's dementia prevention (MAP). https://clinicaltrials.gov/study/NCT04098666
36. 4 Repeat Tauopathy Neuroimaging Initiative (4RTNI). University of California San Franscisco. https://clinicaltrials.gov/study/NCT01804452
37. Bourgeat P, Villemagne VL, Dore V, et al. Comparison of MR-less PiB SUVR quantification methods. *Neurobiol Aging*. 2015;36(Suppl 1):S159-166. doi:10.1016/j.neurobiolaging.2014.04.033
38. Bourgeat P, Dore V, Burnham SC, et al. β-beta-amyloid PET harmonisation across longitudinal studies: application to AIBL, ADNI and OASIS3. *Neuroimage*. 2022;262:119527. doi:10.1016/j.neuroimage.2022.119527
39. Bourgeat P, Dore V, Fripp J, et al. Implementing the centiloid transformation for (11)C-PiB and beta-amyloid (18)F-PET tracers using CapAIBL. *Neuroimage*. 2018;183:387-393. doi:10.1016/j.neuroimage.2018.08.044
40. Iaccarino L, La Joie R, Koeppe R, et al. rPOP: robust PET-only processing of community acquired heterogeneous amyloid-PET data. *Neuroimage*. 2022;246:118775. doi:10.1016/j.neuroimage.2021.118775
41. Whittington A, Gunn RN, Alzheimer's disease neuroimaging I. Amyloid load: a more sensitive biomarker for amyloid imaging. *J Nucl Med*. 2019;60(4):536-540. doi:10.2967/jnumed.118.210518
42. Whittington A, Gunn RN, Alzheimer's disease neuroimaging I. Tau(IQ): a canonical image based algorithm to quantify Tau PET scans. *J Nucl Med*. 2021;62(9):1292-1300. doi:10.2967/jnumed.120.258962
43. Baker SL, Harrison TM, Maass A, La Joie R, Jagust WJ. Effect of off-target binding on (18)F-Flortaucipir variability in healthy controls across the life span. *J Nucl Med*. 2019;60(10):1444-1451. doi:10.2967/jnumed.118.224113
44. Adams JN, Harrison TM, Maass A, Baker SL, Jagust WJ. Distinct factors drive the spatiotemporal progression of tau pathology in older adults. *J Neurosci*. 2022;42(7):1352-1361. doi:10.1523/JNEUROSCI.1601-21.2021
45. Lee WJ, Brown JA, Kim HR, et al. Regional Abeta-tau interactions promote onset and acceleration of Alzheimer's disease tau spreading. *Neuron*. 2022;110(12):1932-1943. doi:10.1016/j.neuron.2022.03.034
46. Young CB, Winer JR, Younes K, et al. Divergent cortical tau positron emission tomography patterns among patients with preclinical Alzheimer disease. *JAMA Neurol*. 2022;79(6):592-603. doi:10.1001/jamaneurol.2022.0676
47. Villemagne VL, Leuzy A, Bohorquez SS, et al. CenTauR: toward a universal scale and masks for standardizing tau imaging studies. *Alzheimers Dement*. 2023;15(3):e12454. doi:10.1002/dad2.12454
48. Leuzy A, Pascoal TA, Strandberg O, et al. A multicenter comparison of [(18)F]flortaucipir, [(18)F]RO948, and [(18)F]MK6240 tau PET tracers to detect a common target ROI for differential diagnosis. *Eur J Nucl Med Mol Imaging*. 2021;48(7):2295-2305. doi:10.1007/s00259-021-05401-4

SUPPORTING INFORMATION

Additional supporting information can be found online in the Supporting Information section at the end of this article.

How to cite this article: Landau SM, Harrison TM, Baker SL, et al. Positron emission tomography harmonization in the Alzheimer's Disease Neuroimaging Initiative: A scalable and rigorous approach to multisite amyloid and tau quantification. *Alzheimer's Dement*. 2025;21:e14378. https://doi.org/10.1002/alz.14378

APPENDIX: ADNI investigators

Name	Location	Role	Contribution
Michael W. Weiner, MD	University of California, San Francisco	Principal investigator	PI
John Q. Trojanowski, MD, PhD	University of Pennsylvania	Core leader	Coordinated biomarker core
Leslie Shaw, PhD	University of Pennsylvania	Core leader	Coordinated biomarker core
Laurel Beckett, PhD	University of California, Davis	Core leader	Coordinated biostatistics core
Paul Aisen, MD	University of Southern California	Core leader	Coordinated clinical core
Ronald Petersen MD, PhD	Mayo Clinic	Core leader	Coordinated clinical core
Andrew J. Saykin, PsyD	Indiana University	Core leader	Coordinated genetics core
Arthur W. Toga, PhD	University of Southern California	Core leader	Coordinated informatics core
Clifford Jack, MD	Mayo Clinic, Rochester, Minnesota	Core leader	Coordinated MRI core
John C. Morris, MD	Washington University	Core leader	Coordinated neuropathology core
William Jagust, MD	University of California, Berkeley	Core leader	Coordinated PET core

Abbreviation: ADNI, Alzheimer's disease neuroimaging initiative.
Scan investigators

Name	Location	Rolen
Susan M Landau, PhD	University of California, Berkeley	POINTER imaging PI
Laura D. Baker, PhD	Wake forest	U.S. POINTER parent trial PI
Mark A. Espeland, PhD	Wake forest	U.S. POINTER main trial PI and biostatistics core
Prashanthi Vemuri, PhD	Mayo Clinic, Rochester	MRI core
Charles DeCarli, MD	University of California, Davis	MRI core
Theresa M. Harrison, PhD	University of California, Berkeley	PET core
Robert A. Koeppe, PhD	University of Michigan	PET core
William J. Jagust, MD	University of California, Berkeley	PET core
Pauline Maillard, MD	University of California, Davis	MRI core
Youngkyoo Jung, PhD	University of California, Davis	MRI core
Laura Lovato, PhD	Wake forest	Biostatistics core
Danielle J. Harvey, PhD	University of California, Davis	Biostatistics core
Arthur W. Toga, PhD	University of Southern California	Informatics core

Note: U.S. POINTER imaging study investigators.

Name	Site	Role
Ezequiel Zamora, MD	Wake forest	Imaging PI
Jo Cleveland, MD	Wake forest	Site PI
Charles DeCarli, MD	University of California, Davis	Imaging PI
Rachel Whitmer, PhD	University of California, Davis	Site PI
Neelum Aggarwal, MD	Rush University	Imaging PI
Christy Tangney, PhD	Rush University	Site PI
Darren Gitelman, MD	Advocate health	Imaging and site PI
Joseph Masdeu, MD, PhD	Houston methodist	Imaging PI
Valory Pavlik, PhD	Baylor College of Medicine	Site PI
Melissa Yu, MD	Baylor College of Medicine	Site PI
Hwamee Oh, PhD	Brown	Imaging PI
Edward Huey, MD	Brown	Imaging PI
Steve Salloway, MD	Butler hospital	Site PI
Rena Wing, PhD	Brown	Site PI

Note: U.S. POINTER imaging site investigators.